

## Cation Sensing by a Luminescent Metal–Organic Framework with Multiple Lewis Basic Sites

Qun Tang,<sup>†</sup> Shuxia Liu,<sup>\*,†</sup> Yiwei Liu,<sup>†</sup> Jun Miao,<sup>†</sup> Shujun Li,<sup>†</sup> Li Zhang,<sup>†</sup> Zhan Shi,<sup>‡</sup> and Zhiping Zheng<sup>\*,§,¶</sup><sup>†</sup>Key Laboratory of Polyoxometalate Science of the Ministry of Education, College of Chemistry, Northeast Normal University, Changchun, Jilin 130024, China<sup>‡</sup>State Key Laboratory of Inorganic Synthesis and Preparative Chemistry, College of Chemistry, Jilin University, Changchun 130012, China<sup>§</sup>Frontier Institute of Science and Technology, Xi'an Jiaotong University, Xi'an, Shaanxi 710054, China<sup>¶</sup>Department of Chemistry, University of Arizona, Tucson, Arizona 85721, United States

## Supporting Information

**ABSTRACT:** A series of novel lanthanide metal–organic frameworks were synthesized using a ligand featuring three carboxylate groups stationed on a triazinyl central motif. The readily accessible multiple Lewis basic triazinyl N atoms allow for complexation of incoming metal ions. Such interactions have been established quantitatively.

Metal–organic framework (MOF) solids are a family of porous materials constructed by the assembly of metal-containing units with appropriate organic linking groups. The ability to tune the pore size and to incorporate various functions into the framework structure offers great promise for the development of materials that are useful for such diverse applications as recognition,<sup>1</sup> separation,<sup>2</sup> and storage of guest molecules of interest,<sup>3</sup> sensing,<sup>4</sup> drug delivery,<sup>5</sup> and catalysis.<sup>6,7</sup>

Among the large number of MOFs,<sup>8,9</sup> those displaying interesting luminescence properties,<sup>10,11</sup> inherent or triggered by interactions with guest species, are receiving increasing current attention because they are useful for the development of sensing technologies among other applications.<sup>4,12–17</sup> Of particular note are lanthanide-containing luminescent MOFs because of the propitious luminescence properties originating from the unique f electronic configurations of these elements. These include extremely sharp emissions and therefore high optical purity, high quantum yields when sensitized by effective ligand-to-metal energy transfer (also known as the “antenna effect”), and structural and compositional optimization of the ligands without affecting the emission characteristics of a chosen lanthanide. More significantly, because of the unique mechanism by which the emissive state of the lanthanide ion is populated, changes of lanthanide luminescence can be effected by a number of means. In this contribution, we report the synthesis, structure determination, and luminescence properties of an Eu<sup>3+</sup>-containing red-emitting MOF. It has been found that the red luminescence of the framework can be significantly enhanced or essentially completely quenched depending on the metal ions that the MOF was in contact with. The study of the relationship between such luminescence changes and the guest–MOF

interactions is of significance for the development of metal-sensing systems.

Our MOF, formulated as [Eu(BTPCA)(H<sub>2</sub>O)]·2DMF·3H<sub>2</sub>O [**1**; H<sub>3</sub>BTPCA = 1,1',1''-(benzene-1,3,5-triyl)tripiperidine-4-carboxylic acid;<sup>18</sup> DMF = dimethylformamide], was synthesized by keeping a mixture of LnCl<sub>3</sub> and H<sub>3</sub>BTPCA in DMF/H<sub>2</sub>O at 65 °C. Isostructural MOFs containing trivalent Ce, Pr, and Nd (2–4) were also obtained under otherwise identical reaction conditions (Table S1 in the Supporting Information, SI). Thermal treatment of **1** removed the aqua ligand and the solvent molecules of crystallization, affording **1a**, putatively the activated form of the porous solid. The powder X-ray diffraction (XRD) pattern of **1a** is nearly identical with that of **1**, indicating that the structural integrity of the framework is maintained (Figure S4 in the SI). As expected, resolution of **1a** in water and DMF afforded respectively **1a**·nH<sub>2</sub>O and **1a**·nDMF, both producing the same XRD patterns as **1** and **1a**. None of these different forms is soluble in water or common organic solvents.

The structure of **1**, shown in Figure 1, was determined by single-crystal X-ray diffraction studies. The electrically neutral

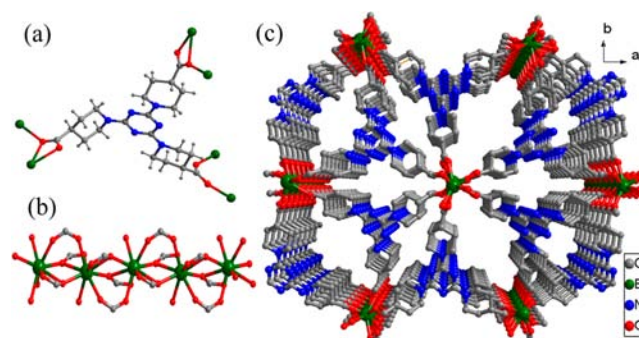


**Figure 1.** (a) Linking of the BTPCA ligand to six different Ln<sup>3+</sup> centers in the title complexes. (b) Chain with nonacoordination for the Ln<sup>3+</sup> coordination environment in the title complexes. (c) Packing of **1** as viewed slightly off the *c* axis. The coordinated water molecules, free solvate molecules, and H atoms were omitted for clarity.

Received: January 6, 2013

Published: March 4, 2013

framework is constructed by  $\text{Eu}^{3+}$  ions bridged by BTPCA ligands. Each BTPCA ligand coordinates six  $\text{Eu}^{3+}$  ions using exclusively its carboxylate groups, two of which are bridging/chelating and the third is bridging with each of its two O atoms coordinating one  $\text{Ln}^{3+}$  ion in a monodentate fashion (Figure 1a). The coordinatively identical  $\text{Eu}^{3+}$  ions are each nonacoordinate and are situated in a coordination sphere composed of nine O atoms from one aqua ligand and six different BTPCA ligands. The bridging interactions are responsible for organization of the metal atoms into a chain structure (Figure 1b) with microporous channels along the crystallographic  $c$  axis (Figures 1c and S5 and S6 in the SI).

The luminescence spectra of  $\text{H}_3\text{BTPCA}$ , the as-synthesized **1**, the thermally activated form **1a**, and the rehydrated form **1a** $\cdot n\text{H}_2\text{O}$  were recorded (Figures S7–S9 in the SI). Upon excitation at 395 nm, **1** luminesces at 590, 618, 650, and 702 nm, characteristic of the  $\text{Eu}^{3+}$  ion and assignable to its  ${}^5\text{D}_0 \rightarrow {}^7\text{F}_n$  ( $n = 1-4$ ) transitions. The ligand-based emission at 445 nm was not observed, indicating that BTPCA is an excellent chromophore for sensitization of the  $\text{Eu}^{3+}$  ion. Thermal treatment of **1** removed the luminescence-quenching aqua ligand and hence the noticeable enhancement in the luminescence of **1a**. Not unexpectedly, rehydration of **1a** to **1a** $\cdot n\text{H}_2\text{O}$  caused significant luminescence quenching. These observations are consistent with the well-established fact that lanthanide luminescence can be effectively quenched through nonradiative decay due to vibronic coupling to high-energy vibrational states of the O–H and N–H bonds.<sup>18</sup>

The Lewis basic triazinyl N atoms of the ligand, directed into the channels of the framework and thus exposed, are supposedly available for interactions with Lewis acidic analytes. Such interactions are expected to alter the electronic structure of the BTPCA ligand that dictates the ligand-to- $\text{Eu}^{3+}$  energy transfer and determines the overall effectiveness of sensitization of the emissive lanthanide ion. Indeed, the samples  $\text{M}^{z+}\text{-1b}$  obtained by immersing **1a** in DMF solutions containing various metal ions displayed markedly different luminescence. As shown in Figure 2, when in contact with  $\text{Fe}^{3+}$ , the red luminescence of **1a** $\cdot n\text{DMF}$ , monitored at 618 nm for the  ${}^5\text{D}_0 \rightarrow {}^7\text{F}_2$  transition, was essentially completely quenched. In stark contrast, the interaction with  $\text{Zn}^{2+}$  drastically enhanced the luminescence intensity, with a maximum of more than 3.5 times as much as that of the parent

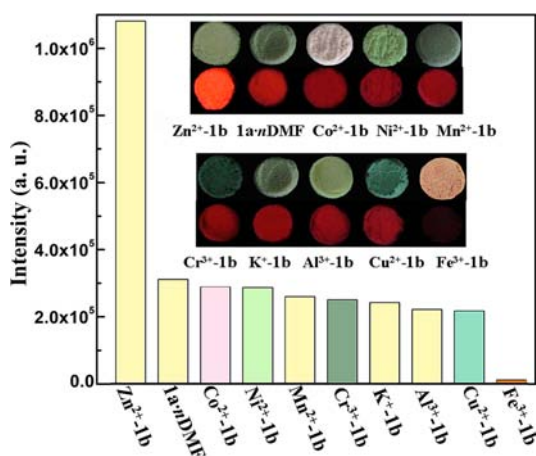


**Figure 2.** Comparison of the luminescence intensity of the  ${}^5\text{D}_0 \rightarrow {}^7\text{F}_2$  transition of  $\text{M}^{z+}\text{-1b}$  versus **1a** $\cdot n\text{DMF}$  ( $\lambda_{\text{ex}} = 344$  nm). The inset shows the photographs of  $\text{M}^{z+}\text{-1b}$  under light and UV-light irradiation.

MOF. The rest of the metal ions ( $\text{K}^+$ ,  $\text{Al}^{3+}$ ,  $\text{Cr}^{3+}$ ,  $\text{Mn}^{2+}$ ,  $\text{Co}^{2+}$ ,  $\text{Ni}^{2+}$ , and  $\text{Cu}^{2+}$ ) tested did not cause any significant change to the intensity of the luminescence (Figures S10–S16 in the SI). Of particular relevance to the present work is  $[\text{Eu}(\text{PDC})_{1.5}(\text{DMF})] \cdot 0.5\text{DMF} \cdot 0.5\text{H}_2\text{O}$  (PDC = pyridine-3,5-dicarboxylate), a luminescent MOF reported by Chen and co-workers.<sup>17</sup> The addition of  $\text{Cu}^{2+}$  led to reduction of the  $\text{Eu}^{3+}$ -originated luminescence to about 50% of its original intensity. The authors speculated that binding of  $\text{Cu}^{2+}$  by the pyridyl N atom of the PDC ligand is responsible because of a compromised antenna effect.

With the hopes of unambiguously establishing the interactions between the metal-ion guests and the MOF host, a series of titration-like experiments were carried out in which the luminescence intensity of the sample obtained by immersing a fixed amount of **1a** in a DMF solution of a specific concentration of  $\text{Fe}^{3+}$  or  $\text{Zn}^{2+}$  was measured. As illustrated by Figure 3a, the

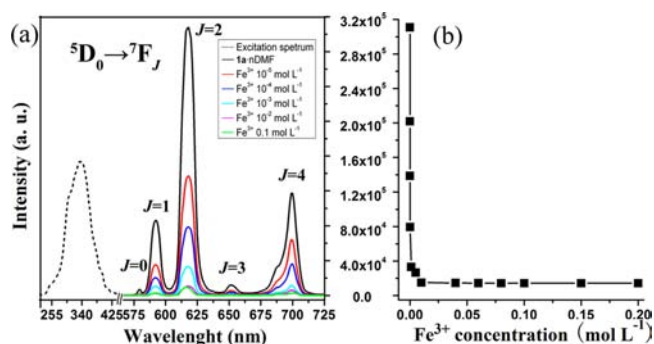


**Figure 3.** (a) Excitation ( $\lambda_{\text{em}} = 618$  nm) and emission ( $\lambda_{\text{ex}} = 344$  nm) spectra of the solid samples of  $\text{Fe}^{3+}\text{-1b}$  obtained by immersing **1a** in DMF solutions with different concentrations of  $\text{FeCl}_3$ . (b) Luminescence intensity of  $\text{Fe}^{3+}\text{-1b}$  monitored at 618 nm versus the concentration of  $\text{Fe}^{3+}$ .

luminescence intensity decreases as the concentration of  $\text{Fe}^{3+}$  increases. Quantitatively, the luminescence was essentially completely quenched when a 3:1  $\text{Fe}^{3+}/\text{1a}$  molar ratio is reached (Figure 3b), clearly suggesting complexation of the luminescence-quenching  $\text{Fe}^{3+}$  with the three triazinyl N atoms of the BTPCA ligand; an increase in the amount of  $\text{Fe}^{3+}$  beyond the equivalence point does not lead to any further changes. The same metal-to-**1a** stoichiometry of 3:1 was obtained by measuring the enhancement of luminescence upon the addition of  $\text{Zn}^{2+}$  (Figures S17 and S18 in the SI), providing further support to the aforementioned of  $\text{M}^{z+}\text{-N}$ (triazinyl) coordination.

The putative sensitization of the  $\text{Eu}^{3+}$  ion for luminescence via energy transfer mediated by the BTPCA ligand is illustrated in Figure 4. The process starts with excitation of the ligand, followed by energy transfer to the emissive states of the  $\text{Eu}^{3+}$  ion. Complexation following the introduction of metal-ion guests into the MOF channels is expected to perturb the electronic structure of the ligand; both the singlet and triplet excited states may be affected. These changes, in turn, will affect how effectively the emissive states of the  $\text{Eu}^{3+}$  ion are sensitized and hence the observed changes in the luminescence intensity.

The diffuse-reflectance UV–visible spectra of **1a** $\cdot n\text{DMF}$  and  $\text{M}^{z+}\text{-1b}$  (Figures S19 and S20 in the SI) suggest that the strong absorption of  $\text{Fe}^{3+}\text{-1b}$  at the excitation wavelength (344 nm) is possibly responsible for the observed quenching of luminescence, which effectively suppresses transfer of the excitation energy to  $\text{Eu}^{3+}$  and therefore population of the emissive states,

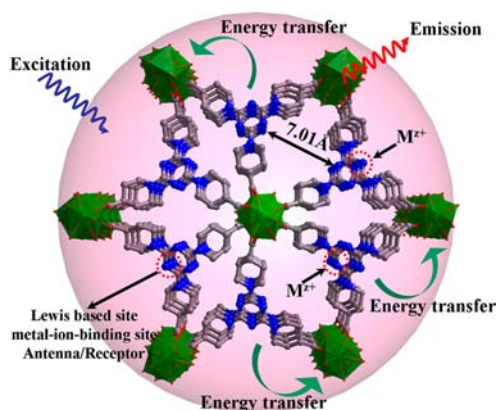


**Figure 4.** Pictorial description of energy-transfer processes, leading to ligand-sensitized  $\text{Eu}^{3+}$  luminescence in the  $\text{Eu}^{3+}$  organic framework **1a**. Legend: green polyhedra,  $[\text{EuO}_8]$ ; gray spheres, C atoms; blue spheres, N atoms.

corroborating the shortest luminescence lifetime of  $\text{Fe}^{3+}$ -**1b** (Figure S25 in the SI). Because the lanthanide-originated luminescence is typically in the micro- to millisecond range, the nanosecond lifetime of the luminescence of  $\text{Fe}^{3+}$ -**1b** clearly indicates that the emissive state of the  $\text{Eu}^{3+}$  ion is essentially unpopulated. In other words, the energy-transfer pathway from the ligand to the emissive center is blocked. In contrast, consistent with the observed significant enhancement of luminescence,  $\text{Zn}^{2+}$ -**1b** displays the weakest absorption at the same wavelength (Table S2 in the SI) and the longest luminescence lifetime (Figure S26 in the SI). As a representative for the other metal ions that do not show significant influence on the luminescence intensity, the decay profile of  $\text{Cu}^{2+}$ -**1b** is shown in Figure S24 in the SI. Not surprisingly, it is very similar to those of **1**, **1a**, and **1a**-nDMF (Figures S21–S23 in the SI). Additionally, the quantum yields for **1a**-nDMF and  $\text{Zn}^{2+}$ -**1b** are 16% and 49%, respectively.

In summary, a luminescent MOF composed of a  $\text{Eu}^{3+}$  ion and a tricarboxylate ligand was synthesized and structurally characterized. Effective sensitization of the metal ion by the ligand is demonstrated. The readily accessible Lewis basic N atoms of the ligand allow for metal–ligand complexation with incoming metal-ion guests. Depending on the nature of the interaction and the resulting perturbation to the electronic structure of the ligand, the efficiency of ligand-to-lanthanide energy transfer is affected, leading to compromised or enhanced population of the lanthanide emissive states and, ultimately, the quenching or enhancement of  $\text{Eu}^{3+}$  luminescence. The essentially complete quenching and drastic enhancement of  $\text{Eu}^{3+}$  luminescence upon the respective incorporation of  $\text{Fe}^{3+}$  and  $\text{Zn}^{2+}$  ions suggest specifically the potential use of the MOF for metal-ion sensing.

## ■ ASSOCIATED CONTENT

### 📄 Supporting Information

X-ray crystallographic data in CIF format, synthesis, characterization, and properties of **1**–**4**. This material is available free of charge via the Internet at <http://pubs.acs.org>.

## ■ AUTHOR INFORMATION

### Corresponding Author

\*E-mail: liusx@nenu.edu.cn (S.L.), zhiping@email.arizona.edu (Z.Z.).

## Notes

The authors declare no competing financial interest.

## ■ ACKNOWLEDGMENTS

This work was supported by the NSFC (Grants 21171032 and 21231002), Fundamental Research Funds for the Central Universities (Grants 09ZDQD0015), and Open Research Fund of the State Key Laboratory of Inorganic Synthesis and Preparative Chemistry (Jilin University, Grant 2012-10).

## ■ REFERENCES

- (1) Ravikumar, I.; Ghosh, P. *Chem. Soc. Rev.* **2012**, *41*, 3077–3098.
- (2) (a) Li, J.-R.; Sculley, J.; Zhou, H.-C. *Chem. Rev.* **2012**, *112*, 869–932. (b) Li, J.-R.; Kuppler, R. J.; Zhou, H.-C. *Chem. Soc. Rev.* **2009**, *38*, 1477–1504.
- (3) (a) Suh, M. P.; Park, H. J.; Prasad, T. K.; Lim, D.-W. *Chem. Rev.* **2012**, *112*, 782–835. (b) Li, J.-R.; Ma, Y.; McCarthy, M. C.; Sculley, J.; Yu, J.; Jeong, H.-K.; Balbuena, P. B.; Zhou, H.-C. *Coord. Chem. Rev.* **2011**, *255*, 1791–1823.
- (4) Kreno, L. E.; Leong, K.; Farha, O. K.; Allendorf, M.; Dwyne, R. P.; Van Hupp, J. T. *Chem. Rev.* **2012**, *112*, 1105–1125.
- (5) Horcajada, P.; Gref, R.; Baati, T.; Allan, P. K.; Maurin, G.; Couvreur, P.; Férey, G.; Morris, R. E.; Serre, C. *Chem. Rev.* **2012**, *112*, 1232–1268.
- (6) (a) Lee, J.; Farha, O. K.; Roberts, J.; Scheidt, K. A.; Nguyen, S. T.; Hupp, J. T. *Chem. Soc. Rev.* **2009**, *38*, 1450–1459. (b) Chen, B. L.; Xiang, S. C.; Qian, G. D. *Acc. Chem. Res.* **2010**, *43*, 1115–1124.
- (7) (a) Wang, Z.; Chen, G.; Ding, K. L. *Chem. Rev.* **2009**, *109*, 322–359. (b) Ma, L. Q.; Abney, C.; Lin, W. B. *Chem. Soc. Rev.* **2009**, *38*, 1248–1256.
- (8) (a) O’Keeffe, M.; Yaghi, O. M. *Chem. Rev.* **2012**, *112*, 675–702. (b) He, Z.; Gao, E.-Q.; Wang, Z.-M.; Yan, C.-H.; Kurmoo, M. *Inorg. Chem.* **2005**, *44*, 862–874. (c) Marchal, C.; Filinchuk, Y.; Imbert, D.; Bünzli, J.-C. G.; Mazzanti, M. *Inorg. Chem.* **2007**, *46*, 6242–6244.
- (9) (a) Kuppler, R. J.; Timmons, D. J.; Fang, Q.-R.; Li, J.-R.; Makal, T. A.; Young, M. D.; Yuan, D.; Zhao, D.; Zhuang, W.; Zhou, H.-C. *Coord. Chem. Rev.* **2009**, *253*, 3042–3066. (b) Bradshaw, D.; Garai, A.; Huo, J. *Chem. Soc. Rev.* **2012**, *41*, 2344–2381.
- (10) (a) Cui, Y. J.; Yue, Y. F.; Qian, G. D.; Chen, B. L. *Chem. Rev.* **2012**, *112*, 1126–1162. (b) Rocha, J.; Carlos, L. D.; Paza, F. A. A.; Ananias, D. *Chem. Soc. Rev.* **2011**, *40*, 926–940.
- (11) (a) Allendorf, M. D.; Bauer, C. A.; Bhakta, R. K.; Houk, R. J. T. *Chem. Soc. Rev.* **2009**, *38*, 1330–1352. (b) Binnemans, K. *Chem. Rev.* **2009**, *109*, 4283–4374. (c) de Lill, D. T.; de Bettencourt-Dias, A.; Cahill, C. L. *Inorg. Chem.* **2007**, *46*, 3960–3965.
- (12) (a) Yanai, N.; Kitayama, K.; Hijikata, Y.; Sato, H.; Matsuda, R.; Kubota, Y.; Takata, M.; Mizuno, M.; Uemura, T.; Kitagawa, S. *Nat. Mater.* **2011**, *10*, 787–793. (b) Jayaramulu, K.; Narayanan, R. P.; George, S. J.; Maji, T. K. *Inorg. Chem.* **2012**, *51*, 10089–10091.
- (13) (a) Chen, B. L.; Yang, Y.; Zapata, F.; Lin, G. N.; Qian, G. D.; Lobkovsky, E. B. *Adv. Mater.* **2007**, *19*, 1693–1696. (b) Xu, H.; Liu, F.; Cui, Y. J.; Chen, B. L.; Qian, G. D. *Chem. Commun.* **2011**, *47*, 3153–3155.
- (14) Wong, K.-L.; Law, G.-L.; Yang, Y.-Y.; Wong, W.-T. *Adv. Mater.* **2006**, *18*, 1051–1054.
- (15) (a) Pramanik, S.; Zheng, C.; Zhang, X.; Emge, T. J.; Li, J. J. *Am. Chem. Soc.* **2011**, *133*, 4153–4155. (b) Lu, Z.-Z.; Zhang, R.; Li, Y.-Z.; Guo, Z.-J.; Zheng, H.-G. *J. Am. Chem. Soc.* **2011**, *133*, 4172–4174.
- (16) Chen, B. L.; Wang, L. B.; Zapata, F.; Qian, G. D.; Lobkovsky, E. B. *J. Am. Chem. Soc.* **2008**, *130*, 6718–6719.
- (17) Chen, B. L.; Wang, L. B.; Xiao, Y. Q.; Fronczek, F. R.; Xue, M.; Cui, Y. J.; Qian, G. D. *Angew. Chem., Int. Ed.* **2009**, *48*, 500–503.
- (18) Zhao, X. L.; He, H. Y.; Hu, T. P.; Dai, F. N.; Sun, D. F. *Inorg. Chem.* **2009**, *48*, 8057–8059.